JOURNAL OF APPLIED POLYMER SCIENCE VOL. IV, ISSUE NO. 12, PAGES 314-331 (1960)

Critical Comparison of Moving Bar Impact with Gas Expansion Machines for Dynamic Loading of Metals

J. M. KRAFFT

Mechanics Division, U. S. Naval Research Laboratory, Washington 25, D. C.

I. INTRODUCTION

To move the grips of a testing machine rapidly apart or together against the resistance of a specimen, two requirements must be met. Obviously the rate of energy input must be sufficient to deform the specimen in a short time; but, more than this, the machine must be stiff enough so that in the face of a rising stress–strain relationship an excessive portion of this energy input is not diverted to storage in the machine rather than utilized to deform the specimen. The storage of energy by a soft machine will reduce the actual strain rate below that nominal for a given rate of energy input or constant-load head speed. Alternately, with a decreasing stress–strain relationship, a soft machine gives up its stored energy and increases the strain rate. This effect is not a small one. Strain-rate variation by a factor of ten is not unusual in gas-pressure high-speed machines loading a ductile tensile specimen. In many metals and, particularly, in some plastics, this variation in straining speed will correspond to a change in flow stress so substantial that it may not be neglected.

In dealing with the strain-rate variation during a dynamic test, it is helpful to be able to predict it. Thus if the characteristics of the machine are understood before it is built, it may be designed to minimize strain rate variation. If the machine is already at hand, an understanding of its dynamic behavior characteristics may still be of assistance in assessing its capabilities and limitations.

Thirdly, in analysis of results, whatever the machine, a knowledge of the strain-rate variation will permit strain rate to be considered as a variable in the stress–strain curve. Accordingly, this paper will discuss the dynamic characteristics of high-speed testing machines as illustrated by two practical types: (*1*) the gas pressure-actuated loader, and (*2*) the bar-impact loader. While the examples illustrating the theory of these machines are taken from tests on steel, they are nonetheless pertinent here, as comparable effects will certainly occur when similar machines are employed for testing plastics.

These two machines represent contrasting methods of rapid load application. In the gas-driven machine, inertial forces, such as those required to accelerate and decelerate the driving piston, are neglected, and the gas pressure applied to the piston is assumed to be immediately applied to the specimen. In the bar method, on the other hand, the inertial forces are of the essence, the operation depending completely upon elastic wave propagation to establish a balance between the deformation rate and the stress at the specimen. This clean-cut distinction is, of course, not accidental. It is only by allowing one of these characteristics to dominate that the analysis of the machines and the processing of data available from them obtains practical simplicity.

The ranges of the two machines are complementary. The gas pressure machines are generally useful at straining speeds under 100 in./sec.; the bar methods are best applied for straining speeds in the range of 1000 in./sec. In the sections to follow, a fairly detailed analysis of the gas machine will be given, as this has not been previously published. The description of the bar method with which it is compared is supported by previous publications and thus will be treated only to the extent necessary for the comparison.

II. EFFECT OF STIFFNESS ON STRAIN RATE IN GAS PRESSURE-DRIVEN MACHINES

For testing machines without inertial effects, there exists a simple general relationship between head speed or actual strain rate and the input speed, the stiffness and specimen characteristics.[1] The stiffness e of such a machine is defined as

$$e = \Delta P/\Delta L \qquad (1)$$

where ΔP is the increment in load required to produce a head displacement increment ΔL. If the load on a testing machine is constant during an input displacement ΔX, then head displacement ΔL will be equal to ΔX. However, if the load increases an amount ΔP as a result of head displacement, only part of ΔX will appear as head displacement, the remainder being accounted for in elastic deflection of the machine;

$$\Delta L = \Delta X - (\Delta P/e) \tag{2}$$

If the testing machine is being used for axial loading of a specimen, the change in load ΔP will be directly proportional to the slope θ of the nominal stress–strain curve ($\theta = d\sigma/d\epsilon$) as given by

$$\Delta P = A_2(\Delta L/L)\theta \tag{3}$$

where A_2 and L are, respectively, the cross-sectional area and initial length of the specimen. By substituting eq. (3) in eq. (2), we may express eq. (2) as:

$$\Delta X = \Delta L + (A_2\Delta L/eL)\theta \tag{4}$$

In the limit and differentiated with respect to time eq. (4) becomes

$$dx/dt = (dL/dt)[1 + (A_2\theta/eL)] \tag{5}$$

or

$$\dot{\epsilon} = (V/L)[1/1 + (A_2\theta/eL)] \tag{6}$$

where $\dot{\epsilon} = (dL/dt)/L$, the nominal strain rate in the specimen, and $V = dx/dt$, the velocity input to the testing machine.

The two requirements of the high speed testing machine are expressed by eq. (6). Given specimen sectional area A_2, length L, and the shape of the stress strain curve θ, then the strain rate $\dot{\epsilon}$ will be dependent only upon the velocity input V and the stiffness e. Analysis of the dynamic characteristics of a machine is in essence a study of factors affecting these two parameters.

The disparity between actual strain rate $\dot{\epsilon}$ and machine input rate V/L may be seen from eq. (6) to increase with increasing specimen area and slope of the stress–strain relationship and to decrease with specimen length L and machine stiffness e. For negative θ values, as will occur during necking of a tensile specimen, θ values comparable to e can cause the strain rate to be multiplied enormously.

In mechanically driven testing machines, the stiffness e may be expected to rise to a somewhat constant value during a test.[2] This is not the case with gas-driven machines, as the stiffness decreases as strain increases at constant load. Consider, for example, a machine of the type illustrated in Figure 1. A pressure source, created by burning a small charge of gunpowder in a chamber of volume v_0 is applied to drive a piston of area A_1 against the resistance to plastic flow offered by a specimen of cross-sectional area A_2. The deformation speed is limited by requiring the gas to pass through a restrictive orifice, a hole of length l and diameter d. The volume displaced by the piston in deforming the specimen a length increment ΔL is ΔLA_1 or v_1; the initial volume on the piston side of the orifice is v_x.

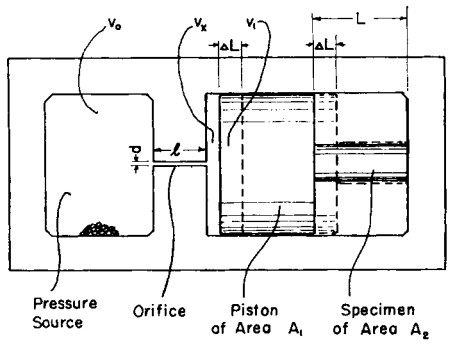

Fig. 1. Schematic representation of gas-pressurized testing machine.

To find the stiffness of the machine of Figure 1, one may substitute for the load $P = p_1A_1$ and for the displacement increment $\Delta L = \Delta v_1/A_1$, whence

$$e = (dp_1/dv_1)A_1^2 \tag{7}$$

For gas machines in which deforming expansion occurs in the order of 10 msec., an assumption of adiabatic conditions is justifiable, in which case

$$pv^\gamma = \text{constant} \tag{8}$$

where γ is the ratio of specific heats.

Substitution of eq. (8) in eq. (7) and differentiation gives

$$e = -\gamma(p_1/v_1)A_1^2 \tag{9}$$

In working with the actual machines, stress and strain will generally be observed rather than pressure and volume, so that it is useful to express eq. (9) in the form

$$e = \frac{\gamma\sigma A_2 L}{[(v_x/A_1L) + \epsilon]} \tag{10}$$

which, when substituted in eq. (6), gives

$$\dot{\epsilon} = (V/L)\frac{1}{1 + [(\epsilon + \epsilon_x)\theta/\gamma\sigma]} \tag{11}$$

where the term v_x/A_1L is considered as equivalent to an initial strain ϵ_x which the initial offset of the piston would produce in the specimen. Considered in this way it is apparent that the stiffness of the gas machine is independent of piston area A_1 but that it is reduced with increased initial volume behind the piston and with increasing strain during the test.

III. EFFECT OF OPERATING PRESSURES ON MACHINE INPUT RATE

The input velocity of the gas machine of Figure 1 will depend directly on the mass flow of gas through the orifice and will not ordinarily be constant throughout a given test. In general, the pressure drop will be so large that the velocity will not vary simply as the square root of the pressure drop but more nearly linearly with the applied pressure as given by the formula[3]

$$w = k[(p_0^2 - p_1^2)d^5]^{1/2}/l \qquad (12)$$

where w is the mass flow of the gas and k is a constant. Experimental evidence will be given later which justifies the assumption that V is proportional to w as given by eq. (12). We need not be concerned with the numerical value of k, as in each test there will be a region of zero slope of the stress–strain curve (θ = O) for which V/L can be found in accordance with eq. (1) from the strain rate $\dot{\epsilon}$ which it then equals. Once a value of V/L is known, it can be used as a match point from which the remaining values can be estimated by assuming functional variation of the form given by eq. (12).

IV. IDEALIZED BEHAVIOR OF GAS-LOADED MACHINE

It is evident from eqs. (11) and (12) that both $\dot{\epsilon}/(V/L)$ and V/L may vary during a test even though p_0 and θ are held constant, a situation representing the most idealized of conditions. Consider the case shown in Figure 2, where p_1 or its stress equivalent rises from half to all of p_0 linearly in 10% strain. If we assume the initial volume v_x behind the piston to be zero, then the strain rate over the speed input $\dot{\epsilon}/(V/L)$ (curve A) is seen to decrease to about 70% of its initial value. The velocity input naturally decreases as the pressure gradient drops, as shown by curve B. The combined effect of A and B is represented by curve C in units of V/L. In real machines, even more variation may be expected, since θ will vary both in magnitude and in sign and p_0 may not be constant

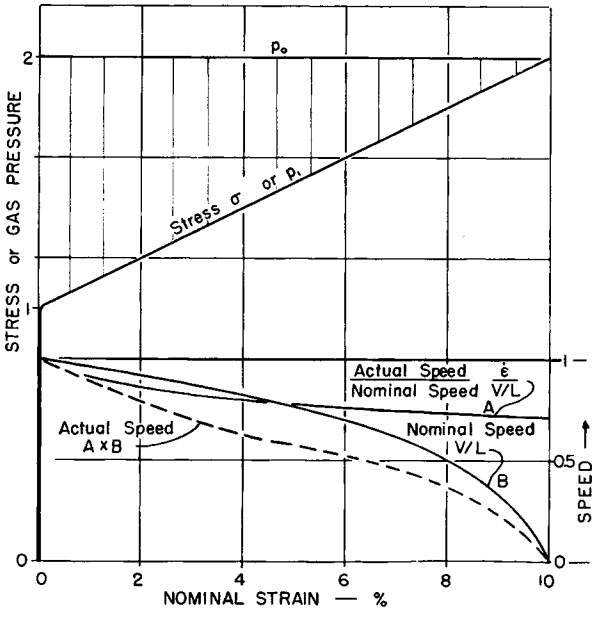

Fig. 2. Characteristic behavior expected from eqs. (11) and (12) of machine shown in Fig. 1 under ideal conditions of constant p_0 and θ(or $d\sigma/d\epsilon$) and with $v_x = 0$.

because the volume v_0 is finite and because of the cooling of the powder-burning gas products.

A practical machine of the type idealized in Figure 1 is illustrated in Figures 3 and 4. Typical oscillograms of load and head displacement versus time are included in Figure 3. Briefly, pressure source p_0 is provided by burning a selected charge of rifle powder in a primed case. The case used, a 300-magnum, 30-caliber case, has a capacity of v_0 of 0.340 in.[3] The case is chambered within a breech block with its open end abutting the orifice hole. The orifice is provided by drilling a small hole axially through a common steel machine screw; the screws are cheap enough to be discarded after a few tests; passage of the hot powder gas tends to erode the orifice in them. The breech block is threaded into one end of a thick-walled steel case which serves as a cylinder for the piston and a rigid loading frame for the specimen. The piston, 1.5 in. in diameter, abuts the breech block at the start of the test so as to minimize the initial volume v_x, thereby providing maximum stiffness for this type machine. The load is weighed with wire resistance strain gages applied longitudinally to a short, hard-steel, anvil rod which is interposed between the piston and the specimen. For compression tests, illustrated in Figure 3, the specimen extends the sectional form ($^1/_2$ in. diameter circle) of the weighing anvil and is fixed at the other end by a base which is threaded into the loading frame

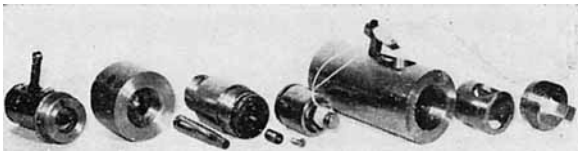

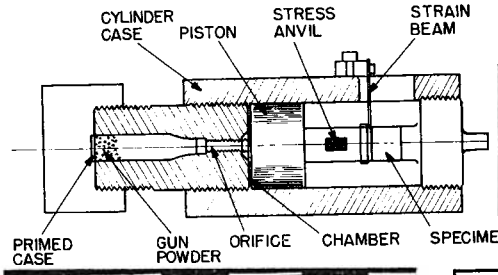

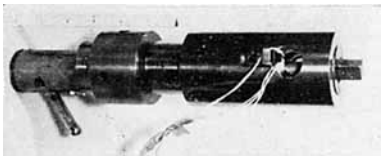

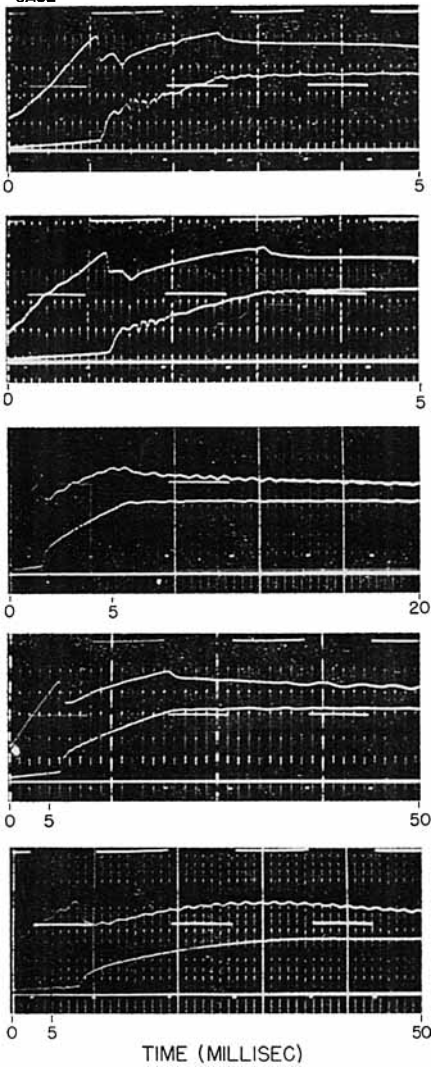

BEFORE YIELD		DURING FLOW	
STRESS RATE	UPPER YIELD STRESS	AT 6% STRAIN	
		STRAIN RATE	STRESS
10^6 LBS/IN^2/SEC	10^3 LBS/IN^2	SEC-1	10^3 LBS/IN^2
61	78	40	67
46	75	34	65
16	68	12	62
9	67	6	61
4	64	1	58

Fig. 3. Schematic diagram and typical records and data on a mild steel for impact bar high speed loader.

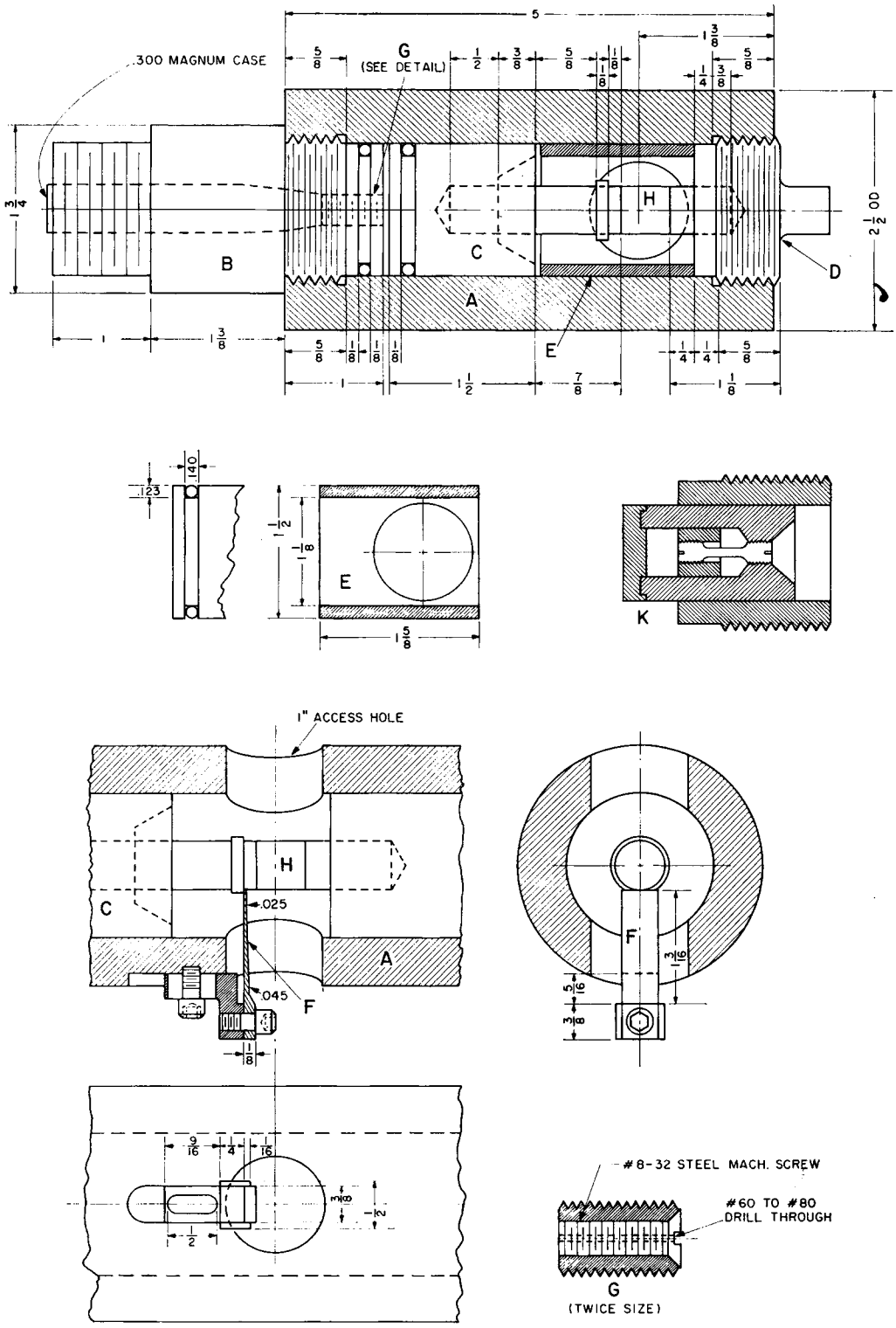

Fig. 4. Details of gunpowder gas-pressurized machine. Note the adapter for small tensile specimens designated K.

cylinder. Motion of the end adjacent to the stress-weighing anvil or the machine head is followed by the deflection of tapered cantilever beam fixed in the loading frame at one end and abutting a slight collar near the end of the stress anvil at the other. The mechanical compliance of this beam (Fig. 4) is sufficient so that its contribution to the force on the stress anvil is negligible, yet its natural frequency with one end resting on the stress anvil is high enough (~3000 cycles/sec.) to permit strain recording with useful accuracy throughout the speed range of this machine. The beam as made of 4340 steel hardened to Rockwell C-45 will permit deflections up to 0.10 in. Head displacement greater than this is prevented by interposition of a limiting collar stop shown in Figure 4.

Wire strain gages attached to opposite faces of the strain beam detect bending strains as a measure of head displacement. These, along with strain signals indicative of load on the weighing anvil, are recorded on suitable cathode-ray oscillograph equipment. One mode of recording, illustrated in Figure 3, utilizes the simultaneous dual traces provided by the electronic switch of a Tektronix type 53/54C preamplifier. Stress is recorded on the upper trace and strain on the lower one at appropriately selected sweep durations as noted. Another technique, of course, is to record stress on one axis, strain on the other of an X–Y oscilloscope, such as will be shown in later examples. A Tektronix type 536 oscilloscope was used for this purpose with timing pulses applied directly to the trace.

This machine was originally designed for compression testing so as to extend the data of the impact bar apparatus. It is, however, adaptable to tensile testing of small specimens by means of the converting adapter shown in Figure 4. This adapter, complete with specimen, is threaded into the end of the loading frame.

The tensile adapter and specimen, like the compression specimen and its base, may be brought to a controlled temperature in a suitable bath prior to the test, then rapidly threaded in and tested. In the compression specimen a short heat buffer disk must be provided between specimen and stress anvil to forestall the quenching of the highly conductive stress anvil for the duration of the test.

V. ANALYSIS OF TESTS WITH THE GAS-DRIVEN LOADER

Equations (11) and (12) provide a basis for calculating head speed expected for a stress–strain relationship as given by the records of the machine. A consistency between calculated and measured machine speed should constitute a validation of the theory. A correct theory should then be one usable for analysis of prospective or of existing machines.

Estimation of the strain rate variation is divided in two steps: (*1*) a calculation of $\dot{\epsilon}/(V/L)$ according to eq. (11), and (*2*) of V/L divided by a reference or match value of V/L according to eq. (12). The product of factors obtained by (*1*) and (*2*) provides the applicable correction factor which when multiplied by the reference strain rate should give the actual strain rate.

Parameters relating to the stress strain curve in eq. (11) are its slope θ, its absolute level σ, and the strain ϵ. All of these are directly readable from the X–Y oscillogram of load versus strain. Calibration traces for the load are provided on each record by periodic insertions (by means of 60 cycle/sec. chopper relay) of resistances in parallel with a strain gage so as to simulate a certain increment in resistance or strain. Independent static calibration on this system is provided occasionally. The strain system is calibrated by comparing the strain residual in each specimen with the breadth of the load–head displacement diagram. Once calibration is established σ, θ, and ϵ can be directly recorded; usually they are tabulated for regular increments of strain ϵ.

The remaining parameters in eq. (11) should be relatively constant. The ratio of specific heats γ is taken here as 1.25, a value typical of the burning products of ordinary gunpowder. A single base nitrocellulose powder of trade designation Dupont 4064 was used. Choice of a powder is not critical nor is the exact value of γ.

The problem remaining now is to measure ϵ_x or the volume between the piston and the orifice as the onset of plastic strain. An estimate is needed under pressure conditions typical of an actual test, as this volume, due to compliance of the O-rings and of the loading frame generally, should increase with pressure or stress level. The procedure adopted consists in burning a fixed charge of powder with the piston blocked at stroke positions varied by unthreading the base anvil. Tracings of pressure time diagrams obtained in such a series are shown in Figure 6. The pressure naturally decreases with time as the powder gas cools. If a set of pressures is read early after burning, effects of unequal cooling should be minimized. Corresponding to each pressure level the volume occupied

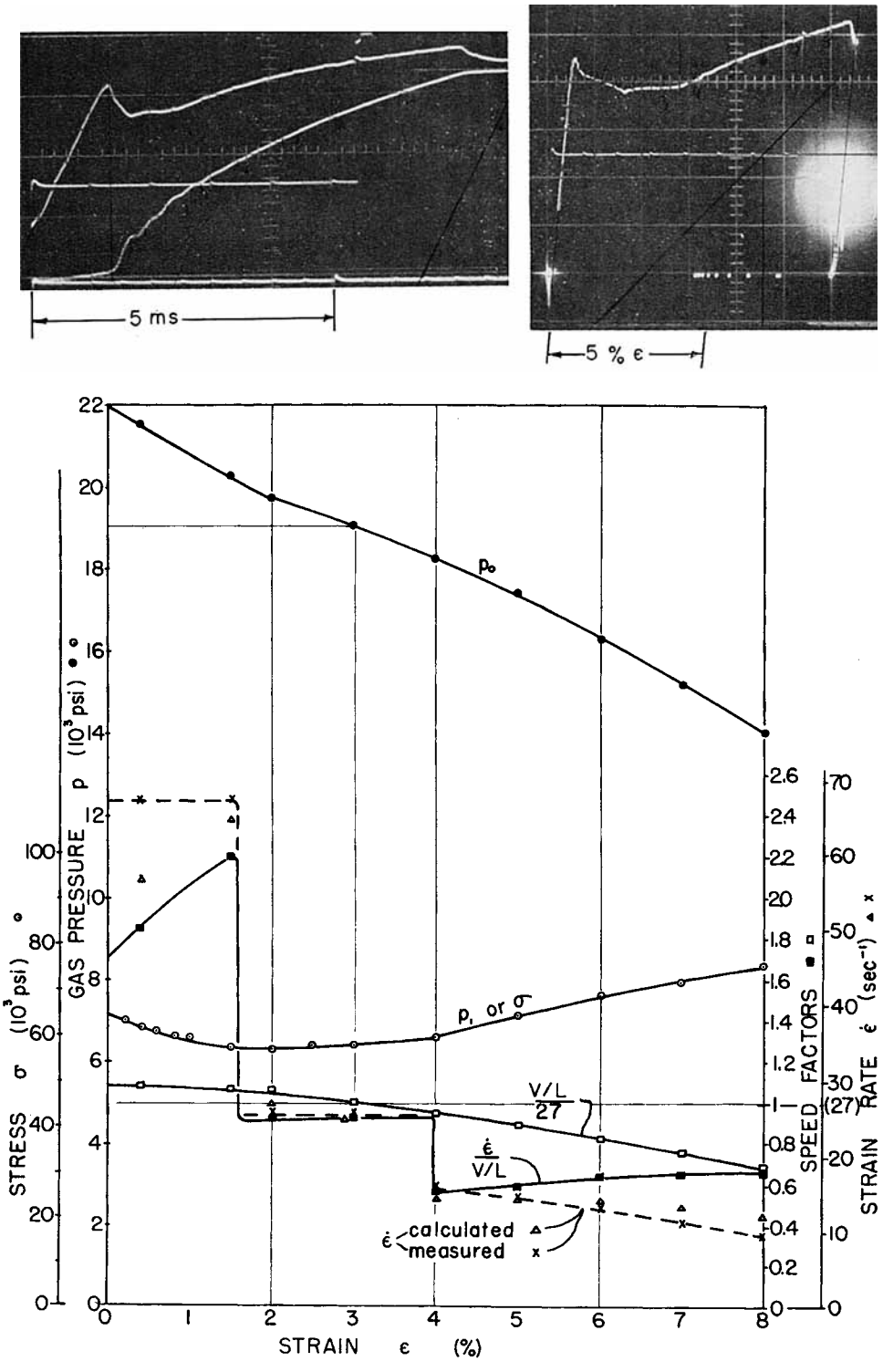

Fig. 5. Records of compression test and results of analysis for strain-rate variation during the test: powder charge 1.1 g.; orifice $d = 0.028$ in., $l = 0.60$ in.; temperature 27°C. (RT); specimen 1010 steel, furnace-cooled 870°C. (see ref. 8 for details) 0.500 in. o.d., 0.925 in. long. Record at left shows load vs. head displacement with X–Y oscilloscope.

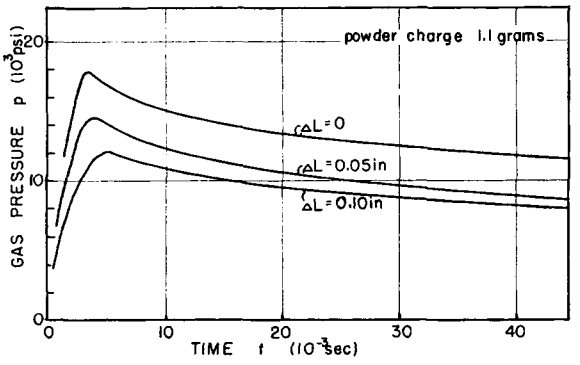

Fig. 6. Pressure from burning 1.1 g. of powder as recorded on machine stress anvil vs. time. The piston was blocked at various stroke positions as noted, and the data are used to determine the volume v_x between orifice and piston when $\Delta L = 0$.

by the burned powder gas should be equal to v_0, the volume of the 300-magnum case (0.340 in.^{3}), plus the unknown volume v_x plus the negative displacement v_1 of the piston in one of its various blocked positions. Again assuming adiabatic conditions, $p(v_0 + v_x + v_1)\gamma$ can be equated for each pair of v_1 values and thus solved for v_x. Insertion of the values indicated in Figure 6 gives an average value for v_x of 0.138 in.^{3} or an equivalent ϵ_x of 8.5% for the 0.925 in.-long specimen used in the tests of Figure 5 and also in those of Figure 8 and 9 to be discussed later.

With parameters determined by the above described procedure, the ratio of $\dot{\epsilon}/(V/L)$ has been calculated and is shown plotted in Figure 5. The

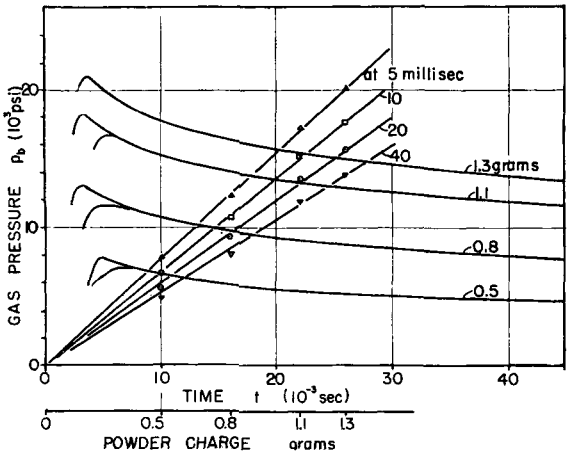

Fig. 7. Pressure from burning varied amounts of powder as noted with piston blocked at $\Delta L = 0$. Note linear pressure vs. powder charge relationship a given time after firing. Left-hand starting curve is for larger orifice (0.040 in.).

strong inverse dependency on θ, the slope of the stress–strain curve, will be noted. The reference or match value of V/L is selected at a point of zero θ. Quite in agreement with the theory, negative θ values show both calculated and measured $\dot{\epsilon}/(V/L)$ ratios greater than unity; positive θ values, ratios less than unity. However, the agreement of calculated and measured speed ratios is not fully satisfactory. It is still necessary to consider the variation in V/L.

To obtain the velocity input or V/L relationship, a measure of the pressure in the case of p_0 is needed. The use of a chemical propellant, while convenient, does introduce a complexity due to the rather rapid pressure drop resulting from conductive cooling of the hot gas, as noted from Figure 6. A theoretical solution to the problem of heat conduction from the gas to the interior surfaces of the machine, while possible, is not necessary. An empirical determination, as shown in Figure 7, is readily obtained. Here, as in Figure 6, the stress-weighing system of the machine has been used to record the pressure–time variation for the piston blocked in its zero stroke position while the weight of gunpowder is varied. The linear plots of pressure at a given time versus weight of powder loading justifies interpolation of these curves to intermediate powder loadings. To determine p_0 and p_1 from such a curve a given time and stroke (i.e., ϵ) after firing, we assume that the product of pv^γ as measured is equal to the sum of this product for case volume and chamber volume. Since chamber pressure p_1 is known from the stress level p_0, the case pressure is determined. This relationship is expressed

$$p_b(v_0 + v_x)^\gamma = p_0(v_0)^\gamma + p_1(v_1 + v_x)^\gamma \quad (13)$$

where p_b is the pressure, measured from Figure 7 a given time after firing (the change in conductive surface area during piston stroke, being relatively small for the large bore stroke ratio, has been neglected here).

Alternately,

$$p_0 = [p_b(v_0 + v_x)^\gamma - p_1(v_1 + c_x)^\gamma]/v_0^\gamma \quad (13a)$$

Values of p_0 obtained from eq. (13) and Figure 7 and of p_1 from the stress record permit evaluation of a factor proportional to V/L, i.e., $(p_0^2 - p_1^2)^{1/2}$ in accordance with eq. (12); all three results are plotted in Figure 5. The product of the V/L and $\dot{\epsilon}/(V/L)$ speed factors should be proportional to the actual straining speed.

The agreement between calculated and measured $\dot{\epsilon}$ (Fig. 5) is thought to be sufficiently close to merit

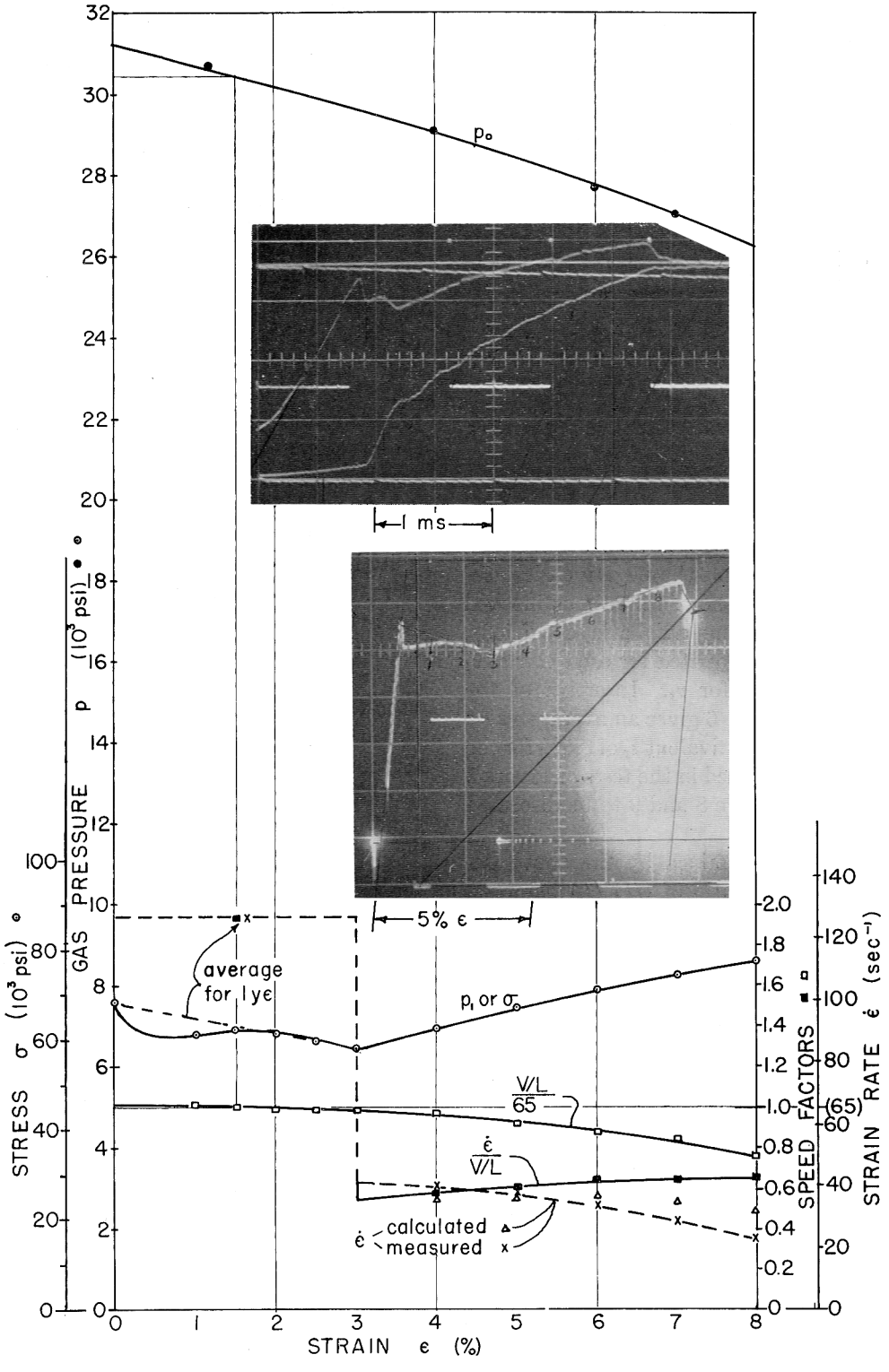

Fig. 8. Analysis of test as shown in Fig. 5 but at higher strain rate: powder charge 1.2 g.; orifice d = 0.040 in., l = 0.60 in.

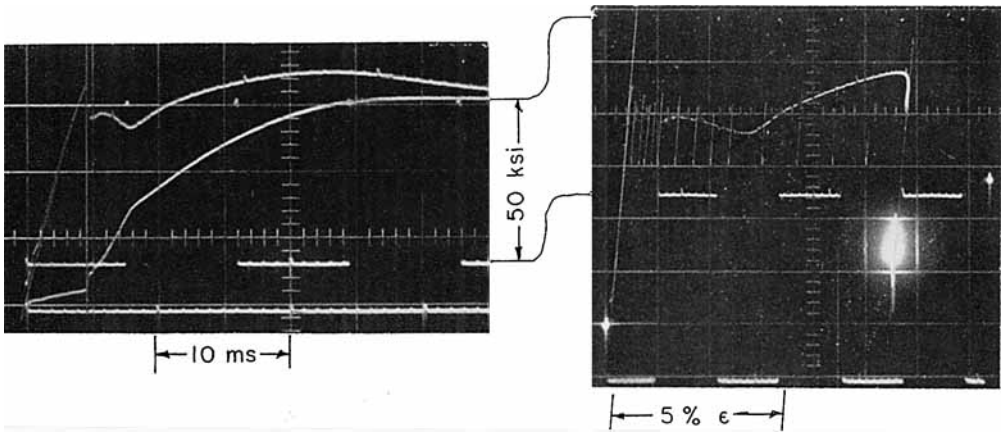

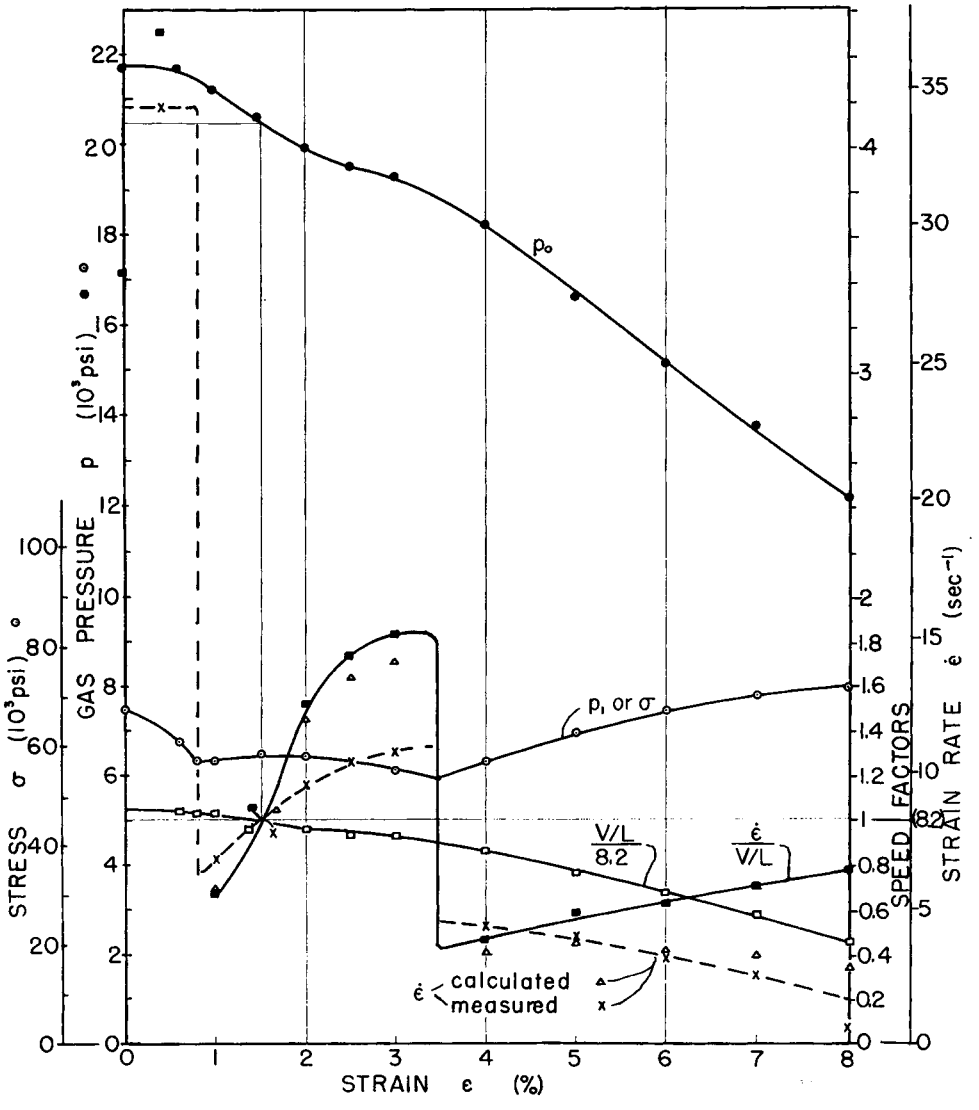

Fig. 9. Analysis of test as shown in Fig. 5 but at lower strain rate: powder charge 1.0 g.: orifice $d = 0.014$ in., $l = 0.25$ in.

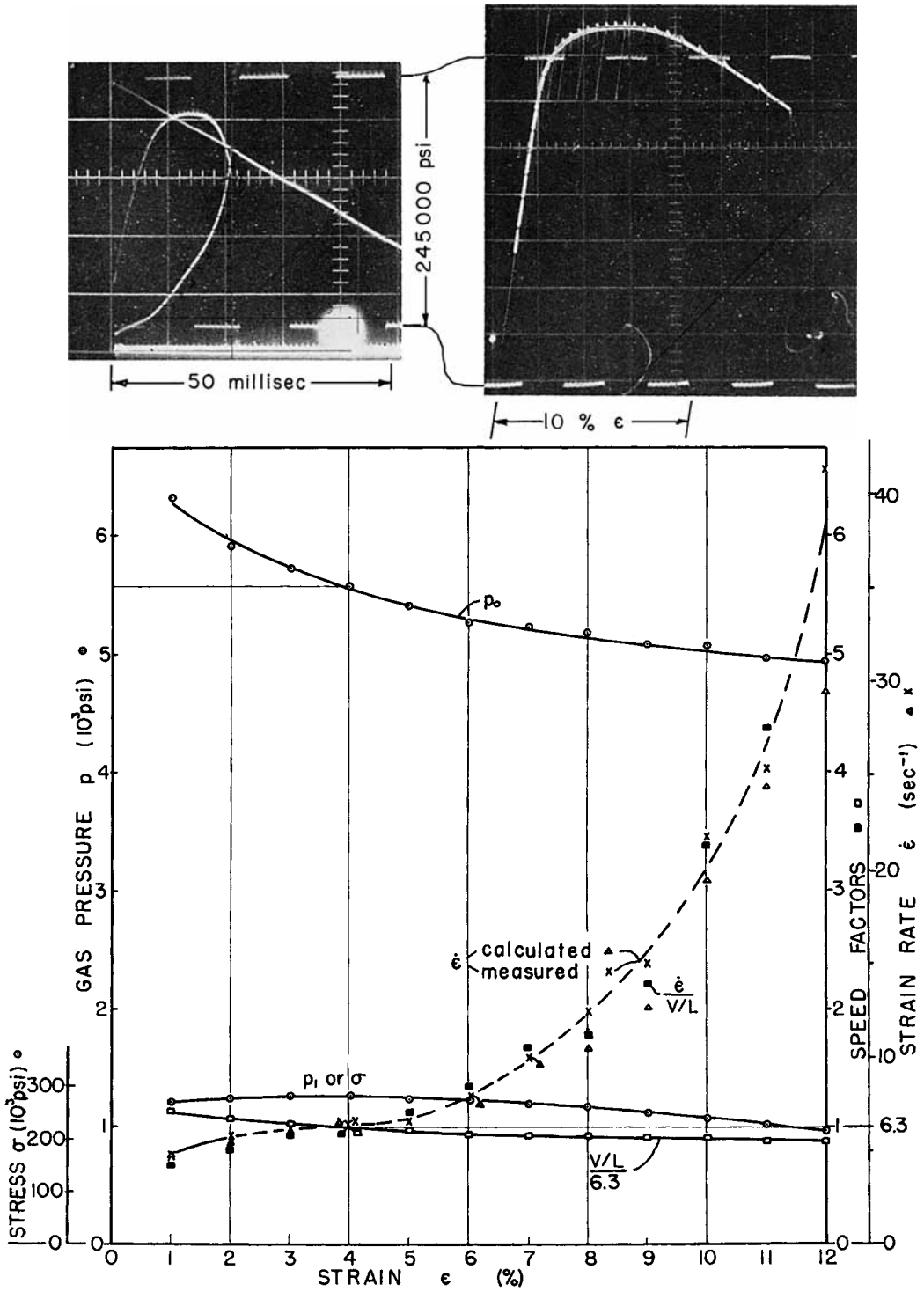

Fig. 10. Records and analysis for tensile specimen using adapter designated K in Fig. 4 and a hollow stress anvil for greater sensitivity: powder charge 0.40 g.; orifice $d = 0.014$ in., $l = 0.25$ in.; $\epsilon_x = 13\%$; specimen 0.100 in. o.d., 0.39 in. active gage length, AMS 6434, 1620°F. oil quench, temper. 400°F., 2 hr. Note that shape of stress-strain curve is not different from that typical of plastics, so that strain-rate variation should also be representative.

confidence for the analysis. At the beginning of strain, the calculated strain rate is most sensitive to v_x, the initial chamber volume adjacent the piston; at higher strain levels, since ϵ_x is not too large, the decrease in velocity input V/L becomes an important term. A correction in V/L (i.e., in p_0) for the increase in cooling surface as the piston moves would put the calculated $\dot{\epsilon}/(V/L)$ in better agreement with measured values at high strain levels.

The data shown in Figure 5 represent a strain rate range intermediate of the capability of the machine (0.028 in. drilled hole orifice; 1.1 g. powder). A similar analysis for a test near the highest speed permitted by strain beam response (0.040 in. drilled hole orifice; 1.2 g. powder) is shown in Figure 8. Here the strain rate variations during the lower yield strain are too rapid to be followed by the strain beam. However, a strain rate computed from average values of θ, σ, and ϵ in this range is in good agreement with the strain rate averaged by the strain beam.

For the other extreme, Figure 9 shows a case approaching the lower speed limit (0.014 in. drilled hole orifice; 1.0 g. powder). Here the speed is low enough to permit the strain beam to follow the undulations in strain rate during the lower yield. The calculated strain rate shows a corresponding variation although the discrepancy in values suggests that the parameter ϵ_x might have been reduced to correspond to the lower operating pressure p_0 for this case. Here, because of the duration of the test, the pressure drop p_0 due to cooling of the powder gas is large, and correspondingly the correction for variation in V/L is important.

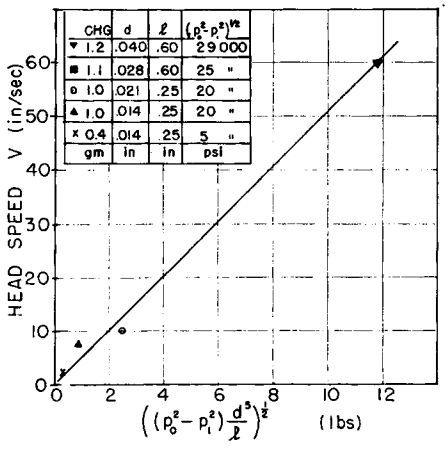

Fig. 11. Plot of head speed V vs. flow rate term suggested for high pressure drop orifice by eq. (12).

The foregoing illustrations pertain to a mild steel with an upper yield point effect in compression. It could be argued that, since such effects do not occur in plastics loaded in tension, the large variations in straining speed would not be a problem. That this is not the case is illustrated in Figure 10, which shows response of the loader to a tensile stress–strain curve (on a high strength steel), quite similar to those typical of plastics. The variation in nominal straining speed approaches a factor of 10 before the specimen is separated. Agreement between calculated and measured strain rate is quite satisfactory.

With accumulation of data of this type, the assumed relationship between the velocity input V and the pressure and orifice parameters can be checked. For the data given in Figures 5, 8, 9, and 10 and from one other case not shown, Figure 11 shows a plot in accordance with eq. (12). The agreement is thought to be compatible with the accuracy of the various measurements and sufficiently close to justify use of eq. (12) or Figure 11 for preliminary design.

VI. BAR-IMPACT LOADERS

In many metals and plastics, a machine head speed of at least 500 in./sec. is permissible without necessitating considerations of plastic wave phenomena. Gas pressure-driven machines, as typified by the gunpowder-pressurized machine described, are not generally capable of head speeds in excess of 100 in./sec. In this particular machine, the response of the strain measuring beam is the primary limitation. This difficulty could be overcome such as by cinematographic or by photoelectric head displacement measurement. Another way would be to express eq. (11) in implicit form as a function of stress rate

$$\dot{\epsilon} = [(V/L)\gamma\sigma - (\int \dot{\epsilon}dt + \epsilon_x)(d\sigma/dt)]/\gamma\sigma \quad (14)$$

and to solve for the strain rate by use of the stress–time record for raw data. However, even if there were success with these alternate approaches, a second limitation would soon be met: that of excitation of the natural frequency of the piston-to-specimen–column mass spring system. For these reasons, a different approach is needed for the higher speed machine. The impact bar loader offers one solution to this problem.

All of the several Hopkinson-loading-bar apparatus developed at NRL for the study of the effects of high-speed straining will permit measurement

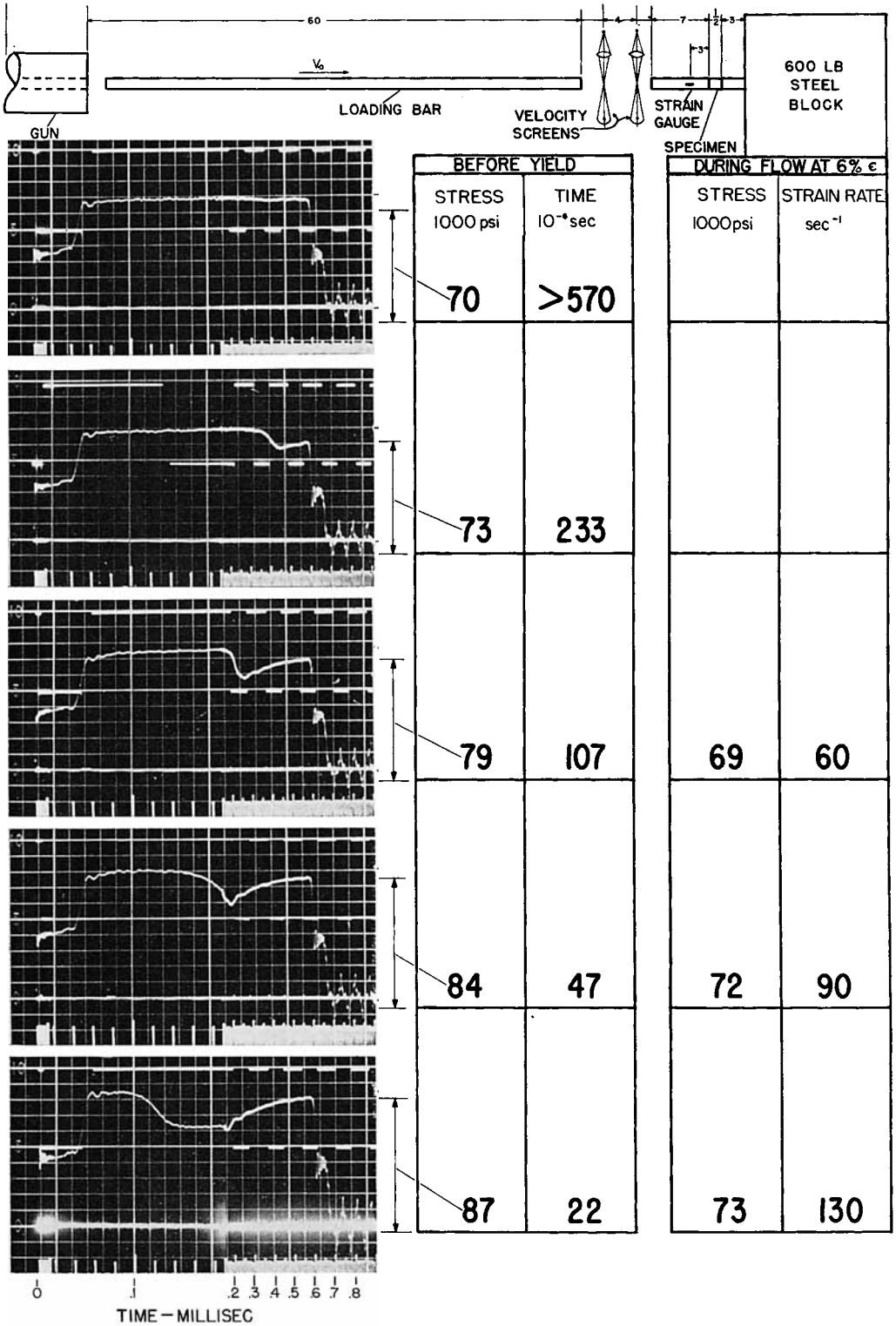

Fig. 12. Schematic diagram and photograph assembled and disassembled of an actual gunpowder gas pressurized machine. Oscillograms show load (upper trace) and head displacement for successively decreasing speed (smaller orifice size) with characteristic data noted at the right.

not only of yield delay, but also of stress during postyield flow as function of time, strain, and strain rate. In all cases, a free, initially unstressed bar of length L_B is accelerated to a constant longitudinal velocity; longitudinal compression is then introduced in the bar by imposing a force on the forward end, which reduces the velocity of this surface with respect to its initial velocity. If the initial velocity V_0 is reduced to zero, as by collision with a rigid infinite-mass anvil, a strain wave of amplitude V_0/C is introduced, traveling away from the impact surface with elastic barwave velocity C. This scheme is used in the apparatus herein described.[6–8] In previous apparatus, the decrease in velocity was affected by impact with another bar of identical diameter and propagation characteristics.[4,5] The resulting velocity decrement was then just one-half that for the fixed anvil, and the corresponding loading strain was correspondingly halved ($V_0/2C$). The pressure corresponding to the strain wave amplitude remains on the impact surface until a wave of unloading returns from the opposite end at time $2L_B/C$ after impact. To use this constant pressure, a specimen of bar diameter is interposed between the colliding bar and the anvil mass. While the specimen remains elastic, a loading stress predictable from the striking velocity V_0 is applied. When the specimen yields, the bar-front velocity increases from zero to that allowed by the plastic compression of the specimen. Thus the rate of convergence between bar and anvil (or average strain rate in the specimen) is directly proportional to the amount by which the stress predicted from the striking velocity is reduced. The stress supported by the specimen while it is so flowing is simply that to which it is reduced. Thus a single stress–time measurement on an elastic bar member adjacent to the specimen provides a measure of stress- and strain-rate versus time, from which a stress–strain relationship is directly integrable.

In essence the apparatus (Fig. 12) differs from that idealized above only in that the specimen is set off from the anvil block by a short elastic bar member so as to allow thermal isolation of the specimen from the block. The hard steel bar, $^1/_2$ in. in diameter and 60 in. in length, is accelerated in the gun and rolls freely in centering guides through velocity screens until it collides with the measuring bar. From the surface of impact, a strain wave of amplitude $V_0/2C$ proceeds backward through the loading bar and forward through the measuring bar. Upon reaching wire strain gages, an oscillographic trace is triggered, whence a strain of amplitude $V_0/2C$ is recorded until the forward wave travels through the specimen to the anvil, is reflected, and finally returns to the gages where it is superimposed on the strain wave still arriving from the loading bar. The duration of double load on the specimen is some 30 μsec. longer than that measured at the gages, owing to the distance separating the two.

The oscillogram tracing (Fig. 13) illustrates constant stress applied to the specimen when the specimen remains elastic. Should yield occur, a pattern typified by Figure 13 results. The plastic strain–time pattern is converted to a stress–strain pattern by numerical integration of the strain rates represented by the differences between patterns A and B, with results as shown in Figure 13.

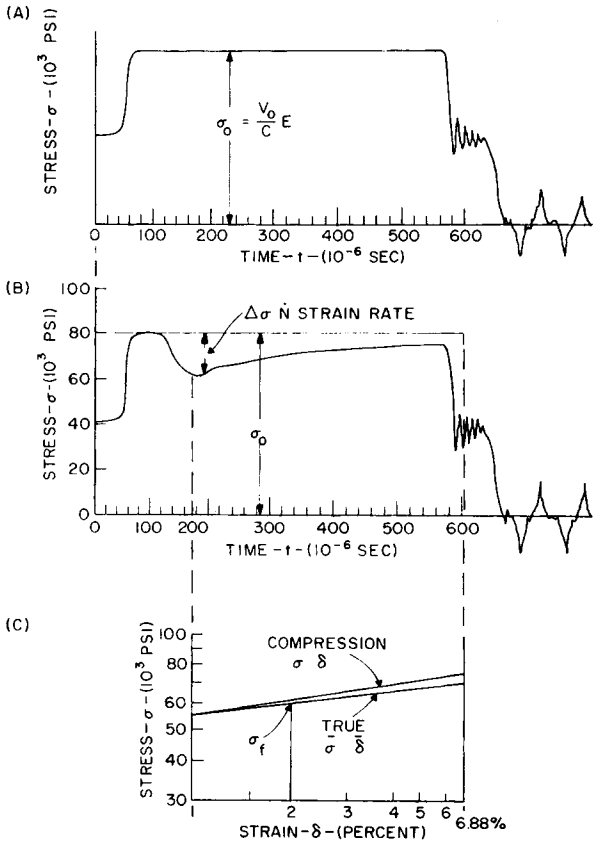

Fig. 13. Typical loading patterns and corresponding stress-strain curves: (A) oscillogram showing loading stress, applied to nonyielding specimen, versus time; (B) oscillogram showing stress, supported by specimen before and during yield process as well as in post-yield plastic flow, vs. time; and (C) plot of stress supported during flow, versus strain measured as timewise summation of differences between (A) and (B) patterns on logarithmic scale (upper curve for engineering compression; lower curve for "true" stress strain).

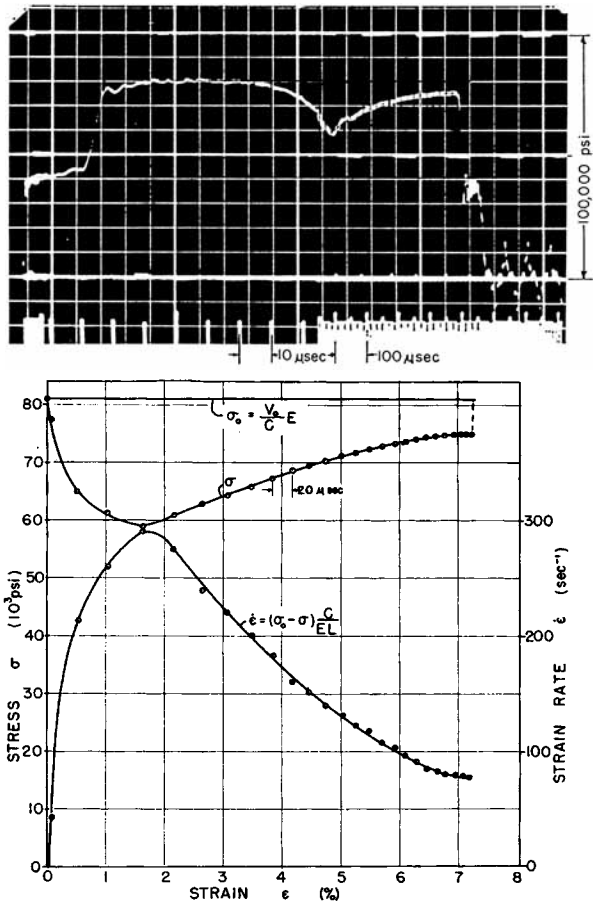

Fig. 14. Typical strain rate variation during bar impact loading. Specimen is 0.500 in. diameter, 0.500 in. length, 1010 steel, as in Figs. 5, 8, and 9.

In the upper curve engineering compressive stress σ versus strain ϵ are plotted on logarithmic scales. The true stress–strain curve shown below it was computed by correcting the stress to allow for increased sectional area.

Additional examples of actual oscillograms for a series with increasing initial striking velocity V_0 are given in Figure 12. Here the initial 10% of the sweep time has been expanded by a factor of 10 (Dumont 329 notch-beam oscillograph) to assist in measurement of the delayed yield effect which is not of interest here. Typical data are illustrated in the tables to the right of the oscillograms in this figure.

It is obvious that strain rate variation is even more inherent in the bar loader than in the gas-driven machine. For the strain rate varies directly as the difference between applied stress σ_0 and the supported stress σ. In any given test, the metal can obtain a stress level, increased by strain hardening and decreased by decreasing strain rate. no greater than σ_0. As it approaches this value, the strain rate is drastically reduced. A typical case in point is shown in Figure 14, where a striking velocity of about 40 ft./sec. produced about 7% plastic strain in a mild steel.

The definition of stiffness applicable to ordinary machines (i.e., $e = \Delta P/\Delta L$) is meaningless for the bar loader. A possible alternative is the quotient

$$e_B = \Delta P/\Delta(dL/dt) \qquad (15)$$

With this as a criterion the stiffness of the fixed-end bar loader would be (EA/C roughly 30 lb./in./sec. for a steel bar of $^1/_2$ in. diameter. A continuous bar system would have half this stiffness, in that the effective head speed corresponding to a given stress drop $\Delta\sigma$ would be twice as large.

The idea of using a tapered bar to back a specimen impacted by a cylindrical bar has been tried as a technique for pacing the rising stress-strain relationship with the stress–time curve. The benefit derived as diminished, however, by the fact that the effective stiffness is continuously increasing in this case from $EA/2C$ to EA/C. Even a constant increment in stress level thus corresponds to a decreasing strain rate. A complexity of record analysis associated with this effect (i.e., the motion of the supporting tapered anvil) further discourages pursuit of this method.

It will be noted that the transient response of the fixed end bar system is limited by the bar length or wave propagation time from specimen to the back-up block. In cases where this limitation is important, the continuous bar system should be considered as a suitable alternative. The fixed-end system has the advantage of requiring only half the impact velocity (one-fourth the energy) to produce a given stress level. The continuous bar system has been used for plastics by Volterra.[9]

VII. COMPARISON OF MACHINES

For high strain-rate studies, the speed range of gas-driven machines tends to complement that of impact bar machines; accordingly the term "comparison" is perhaps not strictly applicable. However, considered with respect to their respective ranges of straining speed, several characteristics might be noted in summary.

Both machines might be termed "soft"; a large variation in strain rate is unavoidable during the test. In the bar an effective "stiffness" $\Delta\sigma/\Delta\epsilon$ is constant and the strain rate depends primarily on

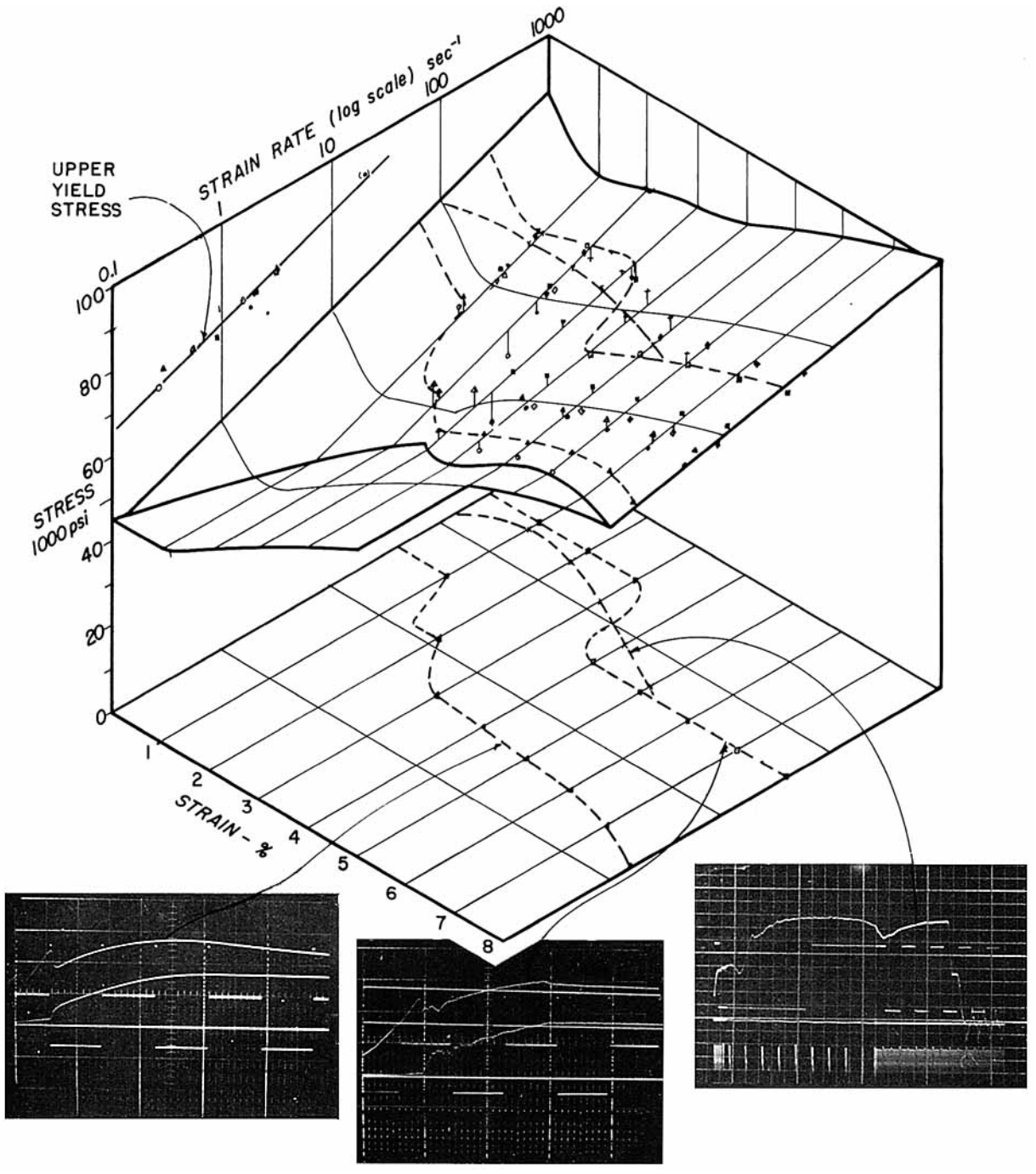

Fig. 15. Correlation of data from both impact bar and powder gas pressurized machines. Note that if strain rate is considered as a variable, reasonable agreement between the data is found. Specimens of a 0.20% C mild steel designated C-3 in. by Krafft and Sullivan.[8]

the stress level. In the gas-loaded machine the stiffness $\Delta P/\Delta L$ decreases as strain increases, and strain rate depends on the shape (slope) of the stress–strain curve and usually to a lesser extent upon the stress level. Analysis of the bar records to obtain stress–strain data is somewhat the more laborious, as a numerical integration of the head speed–time curve is required. With the bar, however, an inherent measure of straining speed is continuously available even at extremely high rates of strain. It would seem fair to say that the machines are about equally desirable in their re-

spective ranges of straining speed. The desirability of either depends on the extent to which strain rate variation can be tolerated.

In mild steel this tolerance is appreciable. For example, Figure 15 illustrates a three-dimensional plot of nominal stress vs. strain vs. strain rate for data obtained with the present machines. The typical variation in strain rate can be noted by traces on the strain vs. strain-rate plane. With the strain rate considered as a variable, good agreement between results from both types of loading is seen to result. It is important to emphasize the converse; misleading interpretations can result from neglect of strain rate variation. History of loading effects which do exist in both metals and plastics are neglected by this type of plot. However, in view of inherent machine characteristics they cannot be properly examined until the primary effects of the instant strain rate have been considered.

References

1. Baron, H. G., *J. Iron Steel Inst. (London)*, **182,** 354 (1956).

2. Fry, L. H., *Proc. ASTM*, **40,** 625 (1940).

3. *Kent's Mechanical Engineers' Handbook*, Power Volume, 12th Ed., Wiley, New York, 1954, pp. 1–24.

4. Krafft, J. M., A. M. Sullivan, and C. F. Tipper, *Proc. Roy. Soc. (London)*, **A221,** 114 (1953).

5. Krafft, J. M., *Proc. Soc. Exptl. Stress Anal.*, **12,** 173 (1955).

6. Krafft, J. M., *Trans. Am. Soc. Metals*, **48,** 249 (1956).

7. Vigness, I., J. M. Krafft, and R. C. Smith, *Proc. Conf. Properties of Materials at High Rates of Strain*, Brit. Inst. Mech. Engrs. London, April 1957.

8. Krafft, J. M., and A. M. Sullivan, *Trans. Am. Soc. Metals*, **51,** 643 (1959).

9. Volterra, E. G., *Proc. U. S. Natl. Congr. Appl. Mech. 2nd Congr.*, 193 (1954).

Synopsis

Achievement of high head speed in a testing machine requires that two conditions be met: (*1*) a high velocity input to the machine, and (*2*) a reasonably high stiffness. The machines discussed here, while excelling in requirement (*1*) are characterized by a rather deficient stiffness. Because of this softness, the strain rate during a test will vary markedly with the amplitude and shape of the stress strain curve; indeed, so much so that it must be considered as a variable in the data. This paper gives an analysis of the motional characteristics of a typical gas-pressurized testing machine. This machine is driven by a pressure source obtained from a chambered burning of gunpowder; head speeds up to 100 in./sec. are reached by a restricted expansion against a piston. It is found that observed strain rate vs. strain behavior can be predicted from the analysis by taking into account the decrease in driving pressure due to gas cooling and to its expansion, and the decrease in stiffness with strain in the specimen or stroke of the piston. Comparison of this type of machine with impact bar loaders previously developed at NRL shows a comparable degree of strain-rate variation for both machines. However, with mild steel, the stress–strain data from the two machines can be correlated by considering instant strain rate as a variable.

Résumé

La réalisation d'une vitesse élevée dans une machine d'essai nécessite deux conditions: (*1*) une introduction rapide dans la machine et (*2*) une rigidité suffisamment élevée. Les machines discutées ici, bien que répondant de facon excellente à la première exigence se caractérisent par une rigidité plutôt déficiente. En conséquence, la vitesse de déformation variera notablement au cours du test avec l'amplitude et la forme des courbes tension–élongation, à telle enseigne que cela introduit une variable en plus dans les résultats. Cet article fournit une analyse des mouvements caractéristiques d'une machine d'essai typique pressurisée au gaz. Cette machine est actionnée par une source de pression obtenue par une chambre à combustion de poudre à canon; des vitesses jusqu'à 100 pouces/sec sont obtenues par une détente limitée contre un piston. La vitesse de déformation en fonction du comportement peut être prédite par analyse des résultats tenant compte de la diminution de la pression due au refroidissement du gaz et à l'expansion de celui-ci et de la diminution de la rigidité avec l'étirement dans l'échantillon ou du coup sur le piston. La comparaison de ce type de machine avec des chargeurs d'impact précédemment mis au point au U. S. Naval Research Laboratory montre une variation de vitesse de déformation semblable dans les deux machines. Toutefois, avec de l'acier doux, les courbes de tension-élongation des deux machines peuvent être reliées en considérant comme variable la vitesse de déformation instantanée.

Zusammenfassung

Die Erreichung einer hohen Geschwindigkeit in einer Prüfmaschine erfordert die Einhaltung zweier Voraussetzungen: (*1*) hohe Geschwindigkeit der Zuführung zur Maschine und (*2*) genügend hohe Steifigkeit. Die Maschinen, die hier diskutiert werden, erfüllen zwar Voraussetzung (*1*) glänzend, sind aber durch eine ziemlich mangelhafte Steifigkeit charakterisiert. Wegen dieser Weichheit wird die Verformungsgeschwindigkeit während eines Tests merklich von der Amplitude und Gestalt der Spannungs-Dehnungskurve abhängen, und zwar so stark, dass sie als Variable bei den Ergebnissen betrachtet werden muss. Die vorliegende Mitteilung gibt eine Analyse der Bewegungscharakteristik einer typischen, mit Gasdruck arbeitenden Prüfmaschine. Die Maschine wird von einer Druckquelle gespeist, die durch eine abgeschlossene Verbrennung von Schiesspulver erhalten wird; Geschwindigkeiten bis zu 100 in/sec werden durch Expansion gegen einen Stempel erhalten. Es wird gefunden, dass das beobachtete Verhalten der Verformungsgeschwindigkeit in Abhängigkeit von der Verformung aus der Analyse vorhergesagt werden kann, wenn die Abnahme des Antriebsdruckes durch Abkühlung und Expansion des Gases und wenn die Abnahme der Steifigkeit mit der Verformung der Probe oder dem Hub des Stempels berücksichtigt wird. Ein Vergleich dieses

Maschinentyps mit den früher im U. S. Naval Research Laboratorium entwickelten Stab-Schlagmaschinen zeigt für beide Maschinen einen vergleichbaren Grad der Änderung der Verformungsgeschwindigkeit. Es können aber bei weichem Stahl die Spannungs-Dehnungsdaten von beiden Maschinen durch Berücksichtigung der momentanen Verformungsgeschwindigkeit als Variabler miteinander in Korrelation begracht werden.

Received April 28, 1960

END OF SYMPOSIUM